Chemistry–A European Journal
Research Article
doi.org/10.1002/chem.202400931
Chemistry Europe
European Chemical Societies Publishing
www.chemeurj.org

Expanding the π-system of Fatty Acid-Anion Transporter Conjugates Modulates Their Mechanism of Proton Transport and Mitochondrial Uncoupling Activity

Edward York,[a] Daniel A. McNaughton,[a] David S. Gertner,[a] Philip A. Gale,[a] Michael Murray,[b, c] and Tristan Rawling*[a]

Mitochondrial uncoupling by small molecule protonophores is a promising strategy for developing novel anticancer agents. Recently, aryl urea substituted fatty acids (aryl ureas) were identified as a new class of protonophoric anticancer agents. To mediate proton transport these molecules self-assemble into membrane-permeable anionic dimers in which intermolecular hydrogen bonds between the carboxylate and aryl-urea anion receptor delocalise the negative charge across the aromatic π-system. In this work, we extend the aromatic π-system by introducing a second phenyl substituent to the aryl urea scaffold and compare the proton transport mechanisms and mitochondrial uncoupling actions of these compounds to their monoaryl analogues. It was found that incorporation of meta-linked phenyl substituents into the aryl urea scaffold enhanced proton transport in vesicles and demonstrated superior capacity to depolarise mitochondria, inhibit ATP production and reduce the viability of MDA-MB-231 breast cancer cells. In contrast, diphenyl ureas linked through a 1,4-distribution across the phenyl ring displayed diminished proton transport activity, despite both diphenyl urea isomers possessing similar binding affinities for carboxylates. Mechanistic studies suggest that inclusion of a second aryl ring changes the proton transport mechanism, presumably due to steric factors that impose higher energy penalties for dimer formation.

Introduction

Cancer cell mitochondria have emerged as a promising target for new anticancer agents due to their key roles in regulating metabolism and cell survival, and because mitochondria in cancerous and noncancerous cells are structurally and functionally distinct.[1–2] In respiring mitochondria, energy derived from nutrient oxidation is used by the electron transport chain (ETC) to pump protons across the mitochondrial inner membrane (MIM) and into the intermembrane space. The resultant mitochondrial membrane potential ($\triangle\Psi_M$) drives proton flow through the MIM-embedded enzyme ATP synthase, which harnesses this energy to synthesise adenosine triphosphate (ATP).[3–4] Thus, nutrient oxidation is coupled to ATP synthesis via the $\triangle\Psi_M$. Mitochondrial uncoupling occurs when protons flow back across the MIM independent of ATP synthase, which dissipates the $\triangle\Psi_M$ and creates a futile cycle of nutrient expenditure without ATP production. Mitochondrial uncoupling can be mediated by MIM-embedded proteins or small molecule mitochondrial uncouplers. Most classical small molecule uncouplers are weakly acidic protonophores that transport protons across the MIM by transmembrane flip-flop of the protonated species followed by deprotonation in the relatively alkaline interior of mitochondria, called the mitochondrial matrix (Figure 1c).[5] For repeated proton shuttling to occur the resulting anion must diffuse across the MIM back into the intermembrane space. To achieve this, the acidic functional group of protonophores is conjugated to a π-system that delocalises the negative charge, generating a lipophilic anion that can permeate through the non-polar core of the MIM. For example, the classical protonophore carbonyl cyanide-4-(trifluoromethoxy)phenylhydrazone (FCCP, **1**, Figure 1a) forms MIM-permeable anions by distributing its negative charge across the hydrazone and aromatic π-systems adjacent to its acidic NH group.[6]

We recently reported the discovery of aryl urea substituted fatty acids (termed aryl ureas, Figure 1a) as a new class of protonophoric mitochondrial uncoupler[7] in which the acidic group is not conjugated to an extended π-system. These compounds utilise an aryl-urea anion receptor to form membrane-permeable dimers that allow for continued protonophoric cycling. As shown in Figure 1c, the carboxylate group of an aryl urea accepts a proton in the intermembrane space and

[a] E. York, Dr. D. A. McNaughton, Dr. D. S. Gertner, Prof. P. A. Gale, Assoc. Prof. T. Rawling
School of Mathematical and Physical Sciences
University of Technology Sydney
Sydney, NSW 2007, Australia
E-mail: Tristan.Rawling@uts.edu.au
[b] Prof. M. Murray
Sydney Pharmacy School, Faculty of Medicine and Health
University of Sydney
Sydney, NSW 2000, Australia
[c] Prof. M. Murray
Woolcock Institute of Medical Research
Macquarie University
Macquarie Park, NSW 2113, Australia

Supporting information for this article is available on the WWW under https://doi.org/10.1002/chem.202400931

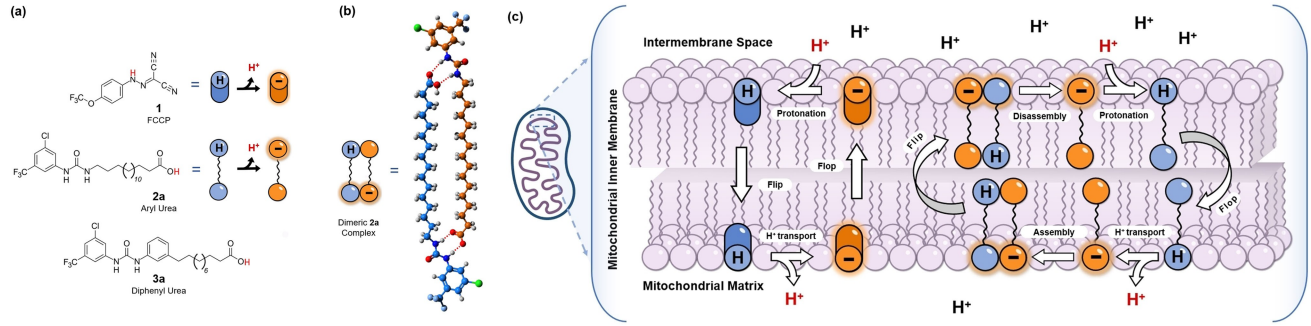

Figure 1. (a) Chemical structures of classical protonophore FCCP (**1**), aryl urea substituted fatty acid (**2a**) and representative diphenyl urea (**3a**) investigated in this work. (b) Ball-and-stick model showing optimised geometry of a monoanionic **2a** dimer calculated at the M062X/6-31 + G(d) level of theory in n-pentadecane, hydrogen bonds shown as red dashed lines. (c) Mechanism of proton transport across the mitochondrial inner membrane (MIM) mediated by FCCP (left) and aryl urea substituted fatty acids (right). The rate determining step is diffusion of the anionic species across the MIM. Left: the acidic group in FCCP is attached to a π-system that delocalises the negative charge to produce a MIM-permeable anion. Right: the acidic group in aryl urea **2a** is separated from its extended π-system by a long alkyl chain, and instead self-assembles into MIM-permeable dimers stabilised by intermolecular hydrogen bonds between the carboxylate and urea moieties. Arrows labelled with "flip" and "flop" denote the transbilayer flip-flop motion of compounds in the MIM as part of the protonophoric cycle.

diffuses across MIM as a neutral species. Deprotonation in the alkaline matrix results in the transport of one proton and generation of an anionic species. The aryl urea then self-assembles into a dimer via intermolecular hydrogen bonds between the carboxylate and urea-based anion receptor (Figure 1b). The MIM-permeable dimer can re-enter the intermembrane space to facilitate further protonophoric cycling. In Figure 1c deprotonation and dimer formation are shown as two distinct events, but it should be noted that these processes may occur in a concerted manner where dimer formation simultaneously drives deprotonation of the acid.

Given their protonophoric activity, the aryl ureas have been assessed as mitochondria-targeted anticancer agents. In cell-based assays the aryl ureas were shown to reduce the viability of several breast cancer cell lines (MDA-MB-231, T47D, MDA-MB-468, and MCF-7), as well as reduce tumour volume in nude mice carrying MDA-MB-231 xenografts.[8] Although the aryl ureas possess promising anticancer actions they lack potency and we have undertaken structural modifications of the scaffold to enhance activity. Attention has focused on the aryl urea-based anion receptor due to its central role in facilitating dimer formation and charge delocalisation across the π-system. Substitution of the aromatic ring with lipophilic electron withdrawing groups (see **2a** in Figure 1a) was found to enhance protonophoric activity by promoting dimer formation and charge delocalisation by through-bond propagation of electron density.[7] Replacement of the anion binding urea group with carbamate groups afforded a series of analogues with similar but not superior activity to the parent aryl ureas.[9]

In this paper we explore the impact of extending the π-system on protonophoric and anticancer activity. To achieve this a series of diphenyl urea substituted fatty acids (termed diphenyl ureas) were synthesised that possess an additional aromatic ring between the alkyl chain and urea binding group (referred to as proximal ring, Figure 1a). The proton transport capacity, mitochondrial actions and anticancer activity of the diphenyl ureas were evaluated and compared to the parent aryl ureas. It was anticipated that extending the aromatic π-system of the urea anion receptor would promote protonophoric activity by increasing the hydrogen bond acidity of the NH groups and the overall surface area available for charge delocalisation. From these studies it emerged that incorporation of *meta*-linked but not *para*-linked proximal rings enhanced proton transport in cell-free HPTS vesicle studies, and the most active compounds depolarised mitochondria, inhibited ATP production and reduced viability of MDA-MB-231 cells with greater potency than their aryl urea counterparts. Using experimental and computational approaches we show that para-linked diphenyl ureas transport protons by a competing fatty acid-activated mechanism due to steric factors that misalign the carboxylate and urea moieties for optimal dimerisation.

Results and Discussion

Compound Library Design

To extend the π-systems of aryl ureas **2a** and **2b** we designed analogues that incorporated a second proximal aromatic ring between the urea and alkyl linker groups (Figure 2). Analogues **3a** and **3b** were designed with alkyl chains connected at the meta-position of the proximal ring. Relative to an unsubstituted phenyl ring, in this position the alkyl chain was expected to donate electron density towards the urea group, which may hinder anion binding and dimer formation.[10] The **4** and **5** series analogues possess ether linkages in the *meta*- and *para*-positions, respectively. Ether substituents provide an electron withdrawing effect in the *meta*-position and a donating effect in the *para*-position.[11] It was therefore anticipated that the urea groups in the **4** series would have higher anion affinity for carboxylates and thus superior protonophoric activity than the **3** and **5** series analogues.

To evaluate the impact of the proximal ring the activities of **3a–5b** were directly compared to the parent compounds **2a** and **2b**. However, introduction of a second ring also increases

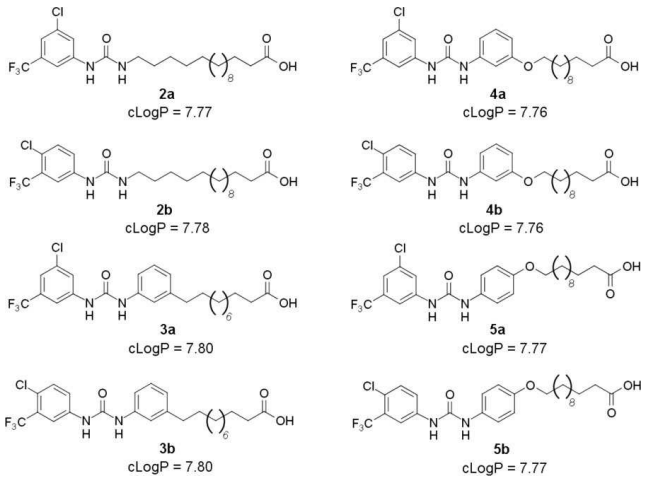

Figure 2. Chemical structures and cLogP values of the aryl and diphenyl ureas studied in this work. The partition coefficient shown represents the average cLogP value obtained using freely available ALOGPS 2.1, XLOGP2 and MiLogP web tools as well as Marvin Consensus software.

compound lipophilicity, which is known to affect anion transport activity.[12] To exclude the role of lipophilicity the length of the alkyl chains in compounds **3a–5b** were shortened to provide compounds with similar calculated LogP (cLogP) values to **2a** and **2b**.

Diphenyl ureas **3-5a** and **3-5b** were synthesised as shown in Scheme 1. Important intermediates in the syntheses were anilines **3-5x**, which could be reacted with carbamoylimidazoles **23a** and **23b** to form the diphenyl urea groups. Ether-linked intermediates **4x** and **5x** were synthesised from bromo-fatty acids **12** and **13**, which were sourced commercially or synthesised from the corresponding alcohol (**11**) using HBr in good yield (87%). The carboxylic acid groups of **12** and **13** were esterified using acetyl chloride in ethanol to give **14** (88%) and **15** (85%), which were then reacted with Boc-protected anilines **19** and **20** under Williamson conditions to yield ethers **Boc4** (40%) and **Boc5** (91%) respectively. The aniline groups of **17** and **18** were Boc protected prior to Williamson reactions to prevent N-alkylation side reactions. **17** was readily Boc-protected by reaction with Boc anhydride in anhydrous dichloromethane, however reactions with **18** under the same conditions gave a mixture of both N- and O-Boc-protected products. Selective Boc protection of **18** was instead achieved using Amberlyst 15 as a catalyst, affording **20** (87%) in high yield.[13] Finally, trifluoroacetic acid was used to remove the Boc groups of **Boc4** and **Boc5** to provide key ether intermediates **4x** (98%) and **5x** (91%) in excellent yields.

A different pathway was needed to produce alkyl intermediate **3x**, which relied on the synthesis of aldehyde **10**. To access **10** the aldehyde group of **6** was first acetal-protected to give **7** in excellent yield (97%). The exposed nitro group was then reduced with Pd/C + $HCOONH_4$ to give aniline **8** (78%). N-Boc protection was achieved in anhydrous dichloromethane under argon to form **9** (71%), followed by selective hydrolysis of the acetal protecting group with Amberlyst 15, at last affording aldehyde **10** (94%). **3x** was then synthesised in four steps from

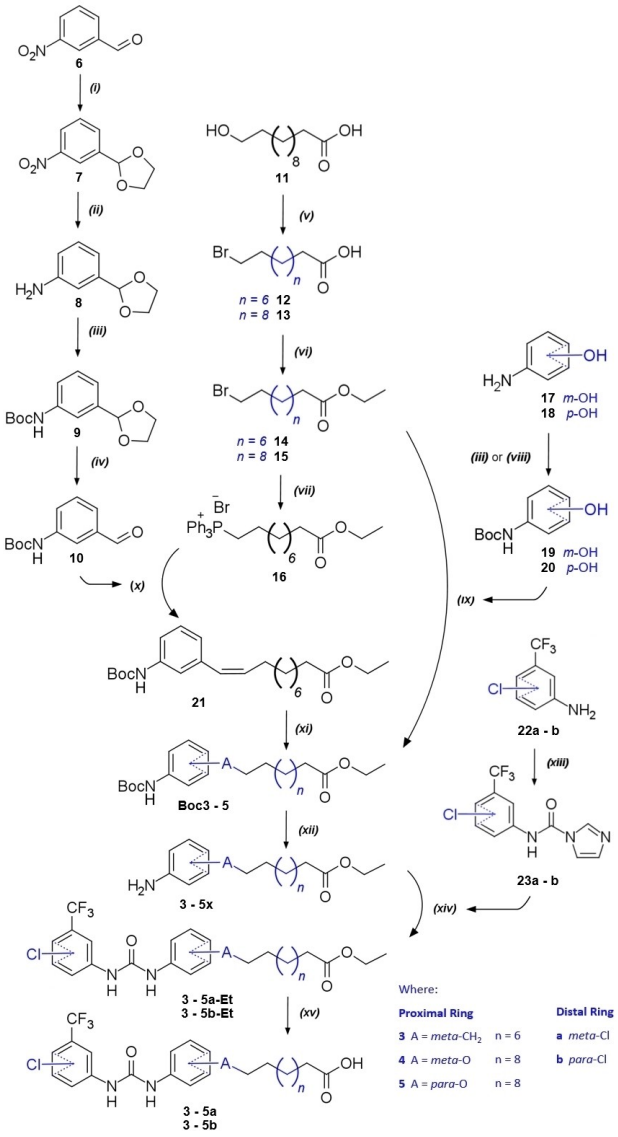

Scheme 1. Synthesis of Diphenyl ureas **3-5a** and **3-5b**. Curved arrows represent convergent syntheses. Reagents and conditions: (i) toluene, ethylene glycol, cat. TsOH, Dean-Stark trap, reflux, 18 h; (ii) absolute ethanol, palladium/charcoal, $HCOONH_4$, 0 °C to 35 °C, 1 h; (iii) anhydrous dichloromethane under argon, Boc anhydride, 40 °C 18 h; (iv) acetone/water, Amberlyst 15, rt, 3.5 h; (v) 1 : 4 98% H_2SO_4 : 48% HBr, reflux, 16 h (vi) absolute ethanol, acetyl chloride, rt, 4 h; (vii) neat, Ph_3P, 120 °C, 20 h; (viii) 95% ethanol, Boc anhydride, Amberlyst 15, rt, 15 min; (ix) anhydrous dimethylformamide under argon, K_2CO_3, 100 °C, 24 h; (x) anhydrous tetrahydrofuran, $NaN(TMS)_2$, 0 °C to −78 °C to rt, 2 h; (xi) absolute ethanol, palladium/charcoal, $HCOONH_4$, 0 °C to 35 °C, 1 h; (xii) anhydrous dichloromethane, trifluoroacetic acid, rt, 4 h; (xiii) 1,2-dichloroethylene under nitrogen, carbonyldiimidazole, 50 °C, 24 h (xiv) anhydrous dichloromethane under argon, rt, 24 h; (xv). 95% ethanol, NaOH, 40 °C, 3 h.

14. In the first step, phosphonium **16** (78%) was synthesised by reaction of **14** with triphenylphosphine. A Wittig reaction between aldehyde **10** and phosphonium **16** with sodium bis(trimethylsilyl)amide was used to prepare olefin **21** (80%),[14] which was reduced to **Boc3** (99%) and then reacted with trifluoracetic acid to remove the Boc group and afford anilino fatty acid ester **3x** (98%).

Following the successful synthesis of key intermediates **3-5x** formation of the diphenyl urea groups was achieved using **23a** and **23b**, which were prepared by reactions of substituted anilines **22a** and **22b** with *N,N'*-carbonyldiimidazole. In solution **23a** and **23b** dissociate into imidazole and isocyanate species,[15] thus serving as masked isocyanates that were reacted with anilino fatty acid esters **3-5x** to give diphenyl urea fatty acid esters **3–5a-Et** and **3–5b-Et** in varying yields (40-90%). In the final step base-catalysed hydrolysis of the ester protecting groups afforded the final acid products **3-5a** and **3-5b** as solids in excellent yields (>90%).

HPTS Proton Transport Assay

The capacity for diphenyl urea fatty acids **3a–5b** to mediate proton transport was assessed using a cell-free 8-hydroxy-1,3,6-pyrene trisulfonic acid (HPTS) vesicular proton transport assay. The results were compared against the activity of aryl ureas **2a** and **2b** to investigate the influence of the proximal ring on transmembrane transport. Large unilamellar 1-palmitoyl-2-oleoyl-*sn*-glycero-3-phosphocholine vesicles (POPC, 200 nm) containing the pH-sensitive fluorophore HPTS were prepared in 4-(2-hydroxyethyl)-1-piperazineethanesulfonic acid (HEPES, 10 mM)-buffered potassium gluconate (100 mM) (see Supporting Information for full experimental details). To initiate the experiment, an addition of base to the extravesicular environment establishes a pH gradient across the membrane before addition of the test molecule. In this system the increase in intravesicular pH by proton transporters can be measured by monitoring the ratio of HPTS fluorescence emission intensity at different excitation wavelengths. Transporter dose-response curves were used to fit an adapted Hill equation and calculate an EC_{50} value for each compound (representing the transporter concentration required to facilitate 50% proton efflux after 200 s). The Hill coefficient, *n*, indicating the stoichiometry of the transport event, was also calculated, and both are presented in Table 1. We note that in this assay proton efflux and hydroxide influx appear identical, which can obscure efforts to identify the transported ion. In 2016 Wu *et al.* suggested that symmetrical bisaryl ureas likely transport OH^- via hydrogen bonds because they lack an acidic group for protonophoric transport.[16] However, the diphenyl ureas studied in this work possess an acidic group, which on deprotonation would anchor the compound to one membrane leaflet and prevent the urea moiety from successfully transporting hydroxide. Consequently, the HPTS transport data was interpreted as extravesicular proton transport. This is supported by the mitochondrial uncoupling activity of the compounds (see following subsection), which requires the transport of protons across the MIM.

Several structure-activity relationships can be gained from the EC_{50} data. Firstly, the **3**- and **4**-series diphenyl ureas are approximately two-fold more potent than parent aryl ureas **2a** and **2b**, while the **5**-series diphenyl ureas were less active. These data indicate that extension of the π-system via proximal ring inclusion can promote proton transport activity, although only when the ring is *meta*-substituted. The data also indicate that 3,5-substitution of the distal ring (**a**-series) is preferred to 3,4-substitution (**b**-series) as the **a**-series diphenyl ureas consistently outperformed their 3,4-substituted counterparts. These trends in activity may be attributed to substituent electronic effects. Due to their substitution pattern the chloro and trifluoromethyl substituents in the **a**-series provide a greater electron withdrawing effect than in the **b**-series ($\sigma_{total} = 0.80$ for **a**-series and 0.66 for **b**-series),[11] which may influence the anion affinity of the urea NHs. Similarly, the reduced activity of **5a** and **5b** may be attributed to the electron donating effect provided by the *para*-ether group on the proximal ring. It should be noted however that the *meta*-alkyl chain of the **3**-series analogues also provides an electron donating effect, but this did not translate to inferior activity compared to the *meta*-ether-linked **4**-series analogues. Alternatively, the diminished activity of **5a** and **5b** could also be due to the subtle shape change between the *meta*- and *para*-linked analogues, which misaligns the carboxylate and urea moieties against favourable dimerisation.

To determine if substituent electronic effects significantly alter the favourability of intermolecular urea-carboxylate interaction, we determined acetate (AcO^-) binding constants using ^{1}H NMR titrations in DMSO-d_6/0.5% H_2O with tetrabutylammo-

Table 1. HPTS (200 s) EC_{50} concentrations and Hill coefficients in Corden Pharma POPC vesicles, acetate binding affinities determined by ^{1}H NMR titrations with tetrabutylammonium acetate (TBAOAc) in DMSO/0.5% H_2O, JC-1 (1 h) and MTS (48 h) absolute IC_{50} concentrations measured in MDA-MB-231 breast cancer cells.

	HPTS EC_{50} (mol%)	Hill (n)	AcO^- Binding Affinity (M^{-1})	JC-1 IC_{50} (μM)	MTS IC_{50} (μM)
2a	0.016 ± 0.003	2.00 ± 0.38	1159 ± 1.4%[a]	2.07 ± 0.05	3.48 ± 0.45
2b	0.021 ± 0.002	1.72 ± 0.25	548 ± 0.8%[b]	2.98 ± 0.10	5.76 ± 0.52
3a	0.008 ± 5×10^{-4}	0.93 ± 0.05	7201 ± 4.8%[b]	0.26 ± 0.05	2.96 ± 0.39
3b	0.013 ± 6×10^{-4}	0.82 ± 0.01	6761 ± 3.8%[b]	0.48 ± 0.04	5.00 ± 0.70
4a	0.008 ± 7×10^{-4}	1.32 ± 0.08	7388 ± 0.7%[b]	0.31 ± 0.01	2.96 ± 0.38
4b	0.011 ± 3×10^{-4}	1.00 ± 0.03	6128 ± 4.1%[b]	0.51 ± 0.06	3.99 ± 0.50
5a	0.023 ± 0.003	1.15 ± 0.09	5077 ± 1.2%[b]	1.75 ± 0.09	5.00 ± 0.90
5b	0.035 ± 0.001	1.33 ± 0.06	6991 ± 4.4%[b]	1.96 ± 0.02	6.95 ± 0.65

[a] Methyl ester tested; [b] Ethyl ester tested.

nium acetate. The methyl or ethyl ester precursors of each compound were used to eliminate competing interactions from their carboxylic acid group. The chemical shifts of the urea NHs were recorded and fit a 1:1 (host:guest) binding model (see Supporting Information for details). Consistent with the EC_{50} data and Hammett substituent constants, **2a**, **3a** and **4a** had higher acetate affinities than their **b**-series counterparts, suggesting the greater electron withdrawing effect of the 3,5-substitution pattern promotes dimerisation and proton transport. However, **5b** bound acetate more strongly than **5a** but exhibited inferior transport activity, opposing this trend. Similarly, the relationship between EC_{50}, Hammett substituent constant and anion affinity was less clear in comparing the **4**- and **5**-series. It was found that all diphenyl ureas bound acetate more strongly than their aryl urea counterparts, but the **5**-series compounds did not have consistently lower anion affinities than the **4**-series despite the electron donating character of the *para*-ether substituent. Taken together, these data indicate that binding affinity alone cannot explain the diminished transport activity of **5a** and **5b**, indicating that the proton transport event is influenced by additional factors.

Interestingly, the HPTS Hill coefficients for the compounds suggest that the proton transport stoichiometry for diphenyl ureas differ from their aryl urea analogues. **2a** and **2b** returned *n* values close to 2 (2.00 and 1.72 respectively). This aligns with previous molecular dynamics simulations that observed **2a** dimer formation between one protonated and one deprotonated **2a** molecule (monoanionic complex),[7] resulting in the transmembrane transport of a single proton. In contrast, the diphenyl ureas returned *n* values between 0.82-1.33, which may reflect that these compounds favour the co-transport of two deprotonated molecules bound at each end (dianionic complex), resulting in a two-proton transport event to give a transport stoichiometry of one. Alternatively, this could indicate that diphenyl ureas transport protons monomerically via intramolecular urea-carboxylate interactions, and/or rely on free fatty acids present in the membrane to facilitate transport. For example, symmetrical bisaryl urea anion transporters have been shown to facilitate proton transport by a fatty acid-activated mechanism, where the transporter shuttles a deprotonated fatty acid across the membrane to enable protonophoric cycling.[10,17] The POPC lipids used for the previous HPTS studies (purchased from Corden Pharma) contain high levels of free fatty acids (up to 2 mol%). Deprotonation of the urea groups in the diphenyl ureas,[18] rather than the carboxylic acid, could also be responsible their proton transport stoichiometry, however this is unlikely. Calculated[19] and experimental[20] pKa values of symmetrical bisaryl ureas substituted with electron withdrawing groups range from 14 to 18, which is significantly higher than known protonophores (pK_a values range from 4 to 8)[5] and indicates that the urea NHs are not sufficiently acidic to allow protonation/deprotonation in HPTS assays and at mitochondrial pH.

To investigate the contribution of the fatty acid-activated mechanism to diphenyl urea proton transport, additional HPTS assays were performed on all compounds using low fatty acid content POPC (purchased from Avanti Polar Lipids) in the presence and absence of oleic acid (OA, at 2 and 4 mol%, see Figure 3). Compounds were tested under each condition at concentrations close to their original EC_{50}. Remarkably, the addition of OA reduced proton transport by all compounds, except for **5a** and **5b**, which showed a sharp increase with the addition of OA. This confirms that **5a** and **5b** transport protons partially by a fatty acid-activated mechanism, which may account for their inferior transport activity. The dual mechanism may stem from steric factors that incur a higher energy penalty for the complexation of para-linked analogues and expose the urea group to the approach of free fatty acids.

To examine this, binding free energies were calculated for the complexation of deprotonated **2a–5a** molecules at the M062X/6-31+G(d) level of theory in *n*-pentadecane to estimate the relative stability of the dimeric and monomeric species in a low dielectric environment such as the MIM (see Supporting Information for details).[21] Notably, deprotonated **5a** molecules dimerised less favourably (−278.5 kJ/mol) compared to meta-linked analogue **4a** (−300.2 kJ/mol), and the same trend was observed for the formation of monomeric species (−283.8 kJ/mol and −321.0 kJ/mol respectively). This indicates that the subtle shape change of para-linked **5a** and **5b** does hinder intra- and intermolecular binding. Both dimerisation and intra-

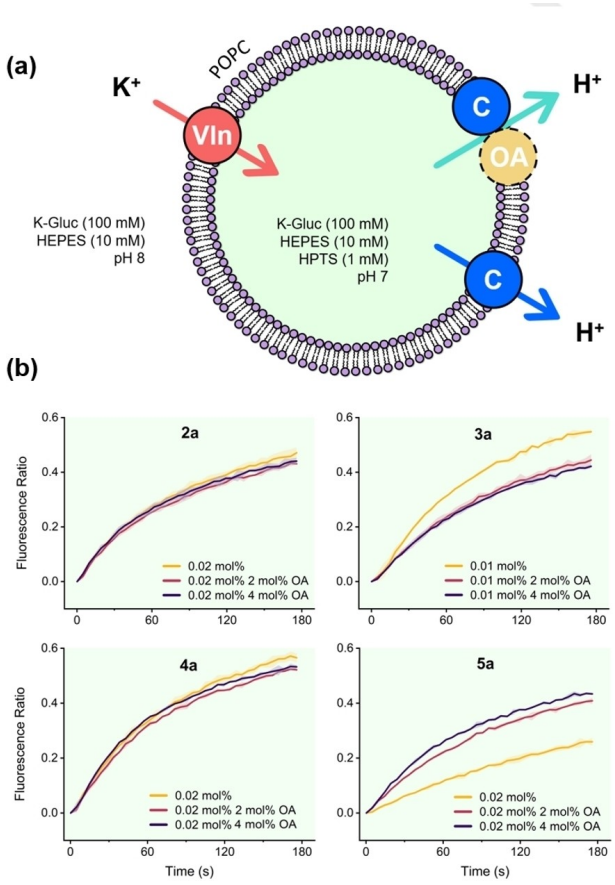

Figure 3. (a) Schematic of the HPTS proton transport assay performed using low fatty acid POPC to determine transporter (C) fatty acid-dependency and (b) the proton transport induced by **2a**, **3a**, **4a** and **5a** in low fatty acid content POPC with and without OA (2 and 4 mol%) (see Supporting Information for **b**-series proton transport plots).

molecular complexation was identified as favourable for all diphenyl ureas **3a–5a** and aryl urea **2a** (Supporting Information, Table S2 and Figure S18), although it should be noted that intramolecular complexation was not observed in previous molecular dynamics simulations of **2a** in DOPC membranes. Instead, the exclusion of the carboxylate group from the bilayer interior favoured linear bilayer packing and the formation of head-to-tail dimers and multimers.[7]

Interestingly, OA addition reduced proton transport for the **3**-series more than the **2**- and **4**-series analogues. HPTS assay Hill analysis of **3a** and **3b** returned the lowest *n* values, which may suggest these compounds exhibit a stricter preference for co-transport as a dianionic complex. This could account for the effect of OA on **3a** and **3b**, as increased competition for urea binding sites would hinder formation of dianionic dimers over cyclic monomers or monoanionic dimers that only require one urea-carboxylate binding event. Taken together, these studies show that the diphenyl ureas operate by different transport mechanisms to the aryl ureas. In contrast to the aryl ureas, all diphenyl ureas transport one proton per molecule. The change in transport stoichiometry may result from the preference of the diphenyl ureas to form dianionic dimers, intramolecularly bound monomeric complexes or complexation to free fatty acids in the membrane, the latter of which is more likely for para-linked analogues **5a** and **5b**.

Mitochondrial Effects of Diphenyl Ureas

We next sought to evaluate the capacity of diphenyl ureas to transport protons across the MIM and depolarise mitochondria in MDA-MB-231 cells. Mitochondrial depolarisation was measured using JC-1, a cationic fluorophore that forms aggregates in energised mitochondria (that possess a high $\triangle\Psi_M$) that fluoresce red.[22] Dissipation of the $\triangle\Psi_M$ by mitochondrial uncouplers releases JC-1 into the cytosol as monomers that fluoresce green. Dose-response curves (Supporting Information, Figure S19) were constructed for all aryl and diphenyl ureas and JC-1 IC_{50} concentrations were determined as the concentration required to shift the red/green fluorescence ratio by 50% of control. Cells were exposed to test compounds for 1 h to distinguish direct mitochondrial uncoupling actions from the characteristic mitochondrial depolarisation that occurs during apoptosis.

As shown in Table 1, all test compounds were active in JC-1 assays. Diphenyl ureas **3a–4b** were the most active compounds in JC-1 assays and shifted the JC-1 red/green fluorescence ratio with IC_{50} concentrations below 1 μM. Para-ether-linked diphenyl ureas **5a** and **5b**, and aryl ureas **2a** and **2b** had similar levels of activity with JC-1 IC_{50} concentrations between 1.75 and 2.98 μM. All **a**-series compounds bearing 3,5-substituted distal rings outperformed their 3,4-substituted **b**-series counterparts. The activity trends observed in JC-1 assays reflect those found in HPTS assays, which indicates that proton transport capacities measured in the vesicle-based HPTS proton transport assay translates into depolarisation of the MIM in live cell mitochondria. Indeed and bivariate analysis of JC-1 and HPTS activity demonstrates a strong positive association ($r^2 = 0.77$, Supporting Information, Figure S21).

Mitochondria utilise the proton gradient across the MIM for ATP production, so we measured ATP levels in MDA-MB-231 cells treated with each compound at the common concentration of 5 μM (see Figure 4). All **3**- and **4**-series compounds, which have submicromolar JC-1 IC_{50} concentrations, reduced intracellular ATP levels to ~80% of time-matched control. Decreased intracellular ATP can result from reduced cell viability rather than direct effects on mitochondrial function, so LDH release assays were conducted to detect cell death. It was found that **3a–4b** (5 μM) did not increase LDH release over 6 h treatment (Supporting Information, Figure S22), thus confirming direct inhibition of ATP synthesis by these compounds. In contrast, aryl urea **2b** and the **5**-series diphenyl ureas failed to reduce ATP production, while **2a** had a modest effect on ATP levels at 4 h only. These compounds all had reduced capacity to depolarise mitochondria in JC-1 assays and their failure to inhibit ATP production at 5 μM is likely to be a result of their diminished proton transport capacity.

Finally, we performed Seahorse Mito Stress Tests using MDA-MB-231 cells treated with the **a**-series compounds to confirm their mitochondrial uncoupling activity. This assay measures the oxygen consumption rate (OCR) of the ETC in MDA-MB-231 cells.

Cells are first treated with the ATP synthase inhibitor Oligomycin, which blocks the flow of protons through ATP synthase. As a consequence electron flow through the ETC is inhibited, which is detected as a decrease in OCR. Introducing a protonophoric uncoupler under these conditions reestablishes proton flow across the MIM, leading to unimpeded ETC activity and an increase in OCR.[23]

Seahorse assays were carried out using **2a**, **3a**, **4a**, **5a** (5 μM) and the classical protonophore **1** (FCCP, 1 μM) for comparison. As shown in Figure 5, **3a** produced an increase in OCR that exceeded that produced by **1**. **4a** and **2a** also increased OCR while compound **5a** showed no effect compared to control.

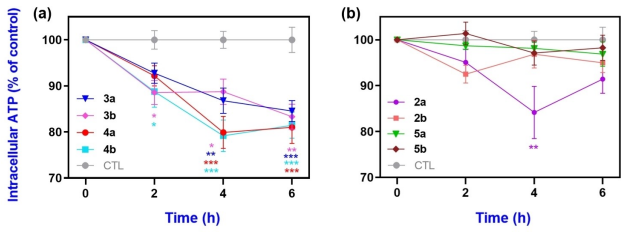

Figure 4. Total intracellular ATP levels in MDA-MB-231 cells following treatment with (a) **3**-, **4**- and (b) **5**-series diphenyl ureas and parent aryl ureas **2a** and **2b** (5 μM). ATP levels are expressed as the percentage of time-matched DMSO control. Different from DMSO-treated control: (*) $P < 0.05$, (**) $P < 0.01$, (***) $P < 0.001$.

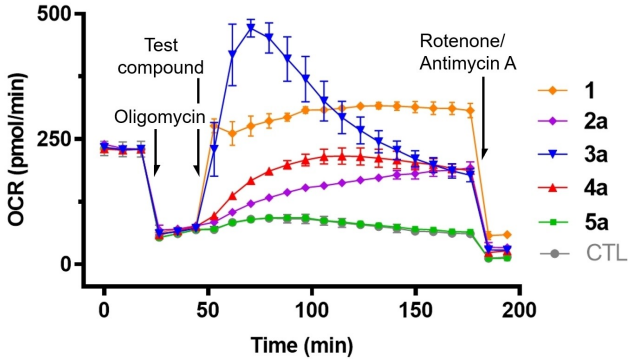

Figure 5. OCR in MDA-MB-231 cells treated sequentially with the ATP synthase inhibitor oligomycin (1 μM), a test compound (5 μM **2a**, **3a**, **4a** or **5a**), and the ETC complex inhibitors rotenone/antimycin A (1 μM). Test compounds were compared against classical protonophore **1** (FCCP, 1 μM) and a 0.1 % DMSO vehicle containing no test compound as control (CTL).

Effects of Diphenyl Ureas on MDA-MB-231 Cell Viability

Mitochondrial uncouplers have been shown to induce cancer cell death so MTS assays were performed to investigate the effect of diphenyl ureas on MDA-MB-231 cell viability. Cells were treated with the test compounds for 48 h over a wide concentration range, and dose-response curves (Supporting Information, Figure S20) were used to calculate absolute IC_{50} concentrations (Table 1). Consistent with the other assays, the **a**-series analogues were more active than their **b**-series counterparts. Bivariate analysis of the HPTS and MTS data exhibits a strong positive association ($r^2 = 0.79$, Supporting Information, Figure S21), although it should be noted that the changes in MTS activities across the test series were minor compared to those seen in JC-1 and HPTS assays. For example, diphenyl urea **3a** was >2-fold more active than **2a** in JC-1 and HPTS assays, but both compounds reduced MDA-MB-231 cell viability with similar IC_{50} concentrations of 2.96 ± 0.39 and 3.48 ± 0.45 μM, respectively.

Taken together, the data presented here demonstrates that incorporation of a *meta*- but not *para*- linked proximal ring into the aryl urea scaffold promotes proton transport capacity in vesicles and live cell mitochondria, but this does not translate into a significant increase in cytotoxicity.

Conclusions

In this paper we extended the π-systems of aryl urea-substituted fatty acids by introduction of a second phenyl group to the scaffold and evaluated the impact on proton transport and mitochondrial uncoupling actions. Incorporation of m*eta*-linked proximal rings into the aryl urea scaffold enhanced proton transport in vesicle studies, indicating improved charge delocalisation by the urea anion binding group to produce membrane-permeable complexes. The most active compounds in the series depolarised mitochondria, inhibited ATP production and reduced cell viability with greater potency than the parent aryl urea analogues. In contrast, diphenyl ureas linked through a 1,4-distribution across the proximal ring showed diminished proton transport and cellular activity, despite both *meta*- and *para*-linked isomers possessing similar binding affinities for carboxylates. Mechanistic testing and computational binding enthalpies indicate that para-linked diphenyl ureas form monomeric and dimeric complexes less favourably due to steric factors and instead transport protons by a competing fatty acid-activated mechanism.

Supporting Information

The authors have cited additional references within the Supporting Information.[24–29]

Acknowledgements

The author acknowledges C. Clarke for his assistance in developing the fatty acid chemistry used in this synthesis, and H. Zeng for her assistance accessing high performance computing workstations for quantum chemistry simulations. E.Y., D.A.M., D.S.G., P.A.G. and T.R. acknowledge and pay respect to the Gadigal people of the Eora Nation, the traditional owners of the land on which we research, teach, and collaborate at the University of Technology Sydney. Open Access publishing facilitated by University of Technology Sydney, as part of the Wiley - University of Technology Sydney agreement via the Council of Australian University Librarians.

Conflict of Interests

The authors declare no conflict of interest.

Data Availability Statement

The data that support the findings of this study are available in the supplementary material of this article.

Keywords: mitochondrial uncoupling · anion transporter · proton transport · dimer · anticancer

[1] S. Fulda, L. Galluzzi, G. Kroemer, *Nat. Rev. Drug Discovery* **2010**, *9*, 447–464.
[2] R. Shrestha, E. Johnson, F. L. Byrne, *Mol. Metab.* **2021**, 101222–101222.
[3] G. M. Cooper, *The Cell: A Molecular Approach. 2nd edition* **2000**.
[4] S. Papa, P. L. Martino, G. Capitanio, A. Gaballo, D. De Rasmo, A. Signorile, V. Petruzzella, *Adv. Exp. Med. Biol.* **2012**, *942*, 3–37.
[5] E. S. Childress, S. J. Alexopoulos, K. L. Hoehn, W. L. Santos, *J. Med. Chem.* **2018**, *61*, 4641–4655.
[6] R. Benz, S. McLaughlin, *Biophys. J.* **1983**, *41*, 381–398.
[7] T. Rawling, H. MacDermott-Opeskin, A. Roseblade, C. Pazderka, C. Clarke, K. Bourget, X. Wu, W. Lewis, B. Noble, P. A. Gale, M. L. O'Mara, C. Cranfield, M. Murray, *Chem. Sci.* **2020**, *11*, 12677–12685.
[8] T. Rawling, H. Choucair, N. Koolaji, K. Bourget, S. E. Allison, Y. J. Chen, C. R. Dunstan, M. Murray, *J. Med. Chem.* **2017**, *60*, 8661–8666.

[9] H. MacDermott-Opeskin, C. Clarke, X. Wu, A. Roseblade, E. York, E. Pacchini, R. Roy, C. Cranfield, P. A. Gale, M. L. O'Mara, M. Murray, T. Rawling, *Org. Biomol. Chem.* **2022**, *21*, 132–139.
[10] E. York, D. A. McNaughton, A. Roseblade, C. G. Cranfield, P. A. Gale, T. Rawling, *ACS Chem. Biol.* **2022**, *17*, 2065–2073.
[11] C. Hansch, A. Leo, S. H. Unger, K. H. Kim, D. Nikaitani, E. J. Lien, *J. Med. Chem.* **1973**, *16*, 1207–1216.
[12] N. J. Knight, E. Hernando, C. J. E. Haynes, N. Busschaert, H. J. Clarke, K. Takimoto, M. García-Valverde, J. G. Frey, R. Quesada, P. A. Gale, *Chem. Sci.* **2016**, *7*, 1600–1608.
[13] F. Jahani, M. Tajbakhsh, S. Khaksar, M. R. Azizi, *Monatsh. Chem.* **2011**, *142*, 1035.
[14] T. Rawling, C. C. Duke, P. H. Cui, M. Murray, *Lipids* **2010**, *45*, 159–165.
[15] T. Rawling, A. M. McDonagh, B. Tattam, M. Murray, *Tetrahedron* **2012**, *68*, 6065–6070.
[16] X. Wu, Luke W. Judd, Ethan N. W. Howe, Anne M. Withecombe, V. Soto-Cerrato, H. Li, N. Busschaert, H. Valkenier, R. Pérez-Tomás, David N. Sheppard, Y.-B. Jiang, Anthony P. Davis, Philip A. Gale, *Chem* **2016**, *1*, 127–146.
[17] X. Wu, P. A. Gale, *J. Am. Chem. Soc.* **2016**, *138*, 16508–16514.
[18] M. Boiocchi, L. Del Boca, D. E. Gómez, L. Fabbrizzi, M. Licchelli, E. Monzani, *J. Am. Chem. Soc.* **2004**, *126*, 16507–16514.
[19] J. Ho, V. E. Zwicker, K. K. Y. Yuen, K. A. Jolliffe, *J. Org. Chem.* **2017**, *82*, 10732–10736.
[20] G. Jakab, C. Tancon, Z. Zhang, K. M. Lippert, P. R. Schreiner, *Org. Lett.* **2012**, *14*, 1724–1727.
[21] Y. Zhao, D. G. Truhlar, *Theor. Chem. Acc.* **2008**, *120*, 215–241.
[22] F. Sivandzade, A. Bhalerao, L. Cucullo, *Bioprocess Biosyst. Eng.* **2019**, *9*, e3128.
[23] A. S. Divakaruni, A. Paradyse, D. A. Ferrick, A. N. Murphy, M. Jastroch, *Methods Enzymol.* **2014**, *547*, 309–354.
[24] M. Cushman, G. Georg, U. Holzgrabe, S. Wang, *J. Med. Chem.* **2014**, *57*, 9219–9219.
[25] G. F. Pauli, B. U. Jaki, D. C. Lankin, *J. Nat. Prod.* **2005**, *68*, 133–149.
[26] A. M. Gilchrist, P. Wang, I. Carreira-Barral, D. Alonso-Carrillo, X. Wu, R. Quesada, P. A. Gale, *Supramol. Chem.* **2021**, 1–20.
[27] F. Neese, *Comput. Mol. Sci.* **2022**, *12*, e1606.
[28] S. F. Boys, F. Bernardi, *Mol. Phys.* **1970**, *19*, 553–566.
[29] S. Simon, M. Duran, J. J. Dannenberg, *J. Chem. Phys.* **1996**, *105*, 11024–11031.

Manuscript received: March 6, 2024
Accepted manuscript online: June 5, 2024
Version of record online: July 31, 2024